Effective Mass of Two-Dimensional ^{3}He

J. Boronat,[1] J. Casulleras,[1] V. Grau,[1] E. Krotscheck,[2] and J. Springer[2]

[1]*Departament de Fisica i Enginyera Nuclear, Campus Nord B4-B5, Universitat Politécnia de Catalunya, E-08034 Barcelona, Spain*

[2]*Institut für Theoretische Physik, Johannes Kepler Universität, A 4040 Linz, Austria*

(Received 12 June 2003; published 21 August 2003)

We use structural information from diffusion Monte Carlo calculations for two-dimensional ^{3}He to calculate the effective mass. Static effective interactions are constructed from the density and spin-structure functions using sum rules. We find that both spin and density fluctuations contribute about equally to the effective mass. Our results show, in agreement with recent experiments, a flattening of the single-particle self-energy with increasing density, which eventually leads to a divergent effective mass.

DOI: 10.1103/PhysRevLett.91.085302 PACS numbers: 67.57.Pq

Two-dimensional liquid ^{3}He is particularly interesting because it is, even at zero temperature, not self-bound and can, therefore, be studied in a wide density range. Although governed by one of the simplest Hamiltonians for realistic many-body systems, ^{3}He exhibits a wide range of delicate and complex phenomena which have, by and large, been resilient to an understanding from the underlying Hamiltonian. Only recently, Monte Carlo techniques have moved to a point where structural properties have been understood from first principles [1,2].

Low-energy dynamical properties of ^{3}He at low temperatures are phenomenologically described by Landau's Fermi-liquid theory, which establishes relationships between observable quantities such as the specific heat, the compressibility, and the magnetic susceptibility. Understanding the so-called Fermi-liquid parameters in ^{3}He has therefore been a recurring issue in theoretical low-temperature research. The calculation of Fermi-liquid parameters in terms of Feynman diagrams is operationally well defined, but the execution of the theory from an underlying microscopic Hamiltonian is far too complicated to be practical. Hence, many attempts have been made to explain the features of Fermi-liquid parameters within semiphenomenological models [3–5].

We examine in this Letter physical effects contributing to the effective mass in two-dimensional ^{3}He. This work is motivated by a recent sequence of measurements [6] that seem to indicate a Mott-Hubbard transition in quasi-two-dimensional ^{3}He atomic monolayers. Technically, our calculations correspond to those of Refs. [7,8], but we use as much information as possible from accurate ground state Monte Carlo simulations.

The relevant quantity for the effective mass is the single-particle propagator $G(k, \omega)$ in the vicinity of the Fermi surface. It is expressed in terms of the proper self-energy $\Sigma^*(k, \omega)$ through the Dyson equation [9]

$$G_{\sigma\sigma'}(k, \omega) = \frac{\delta_{\sigma\sigma'}}{\hbar\omega - t(k) - \Sigma^*(k, \omega)}; \tag{1}$$

$t(k) = \hbar^2 k^2/2m$ is the free single-particle spectrum. The physical excitation spectrum is obtained by finding the poles of the Green's function in the (k, ω) plane. Several steps are involved in constructing practically useful expressions for the proper self-energy $\Sigma^*(k, \omega)$. The first step is the derivation of effective interactions. We use for that purpose results from diffusion Monte Carlo calculations [2]. The structure function can be written as

$$S(k) = S_\rho(k) + S_\sigma(k)\boldsymbol{\sigma}_1\boldsymbol{\sigma}_2, \tag{2}$$

where the components are constructed from the structure functions for parallel and antiparallel spins. Both quantities are obtained by either directly evaluating the expectation value of $\rho_{\mathbf{k}}\rho_{-\mathbf{k}}$ or by Fourier transforming the corresponding pair distribution functions. The first procedure is more accurate for long wavelengths up to the size of the simulation box, whereas the latter is appropriate for medium and short wavelengths. Moreover, one can determine the long-wavelength limit of $S_\rho(k)$ from the bulk compressibility; we comment on this below. We have taken the Fourier transform of the pair distribution function for wave numbers $k \geq k_F$ and direct simulation data for long wavelengths and have smoothly interpolated these data towards $k \to 0$. The static structure functions at two densities are shown in Fig. 1. The density static structure function shows the typical behavior, whereas the spin-structure function depends only weakly on the density in the most interesting regime.

The static structure functions are related to the dynamic response functions through the m_0 sum rule

$$S_s(k) = -\int_0^\infty \frac{d(\hbar\omega)}{\pi} \mathrm{Im}\chi_s(k, \omega). \tag{3}$$

Above, $s \in \{\rho, \sigma\}$ refers to the spin channel. Assuming a model such as the random phase approximation (RPA),

$$\chi_s(k, \omega) = \frac{\chi_0(k, \omega)}{1 - \tilde{V}_s(k)\chi_0(k, \omega)}, \tag{4}$$

we can relate the static structure functions $S_s(k)$ uniquely to the effective interactions $\tilde{V}_s(k)$. The tilde in the potential indicates that we use dimensionless Fourier transforms, $\tilde{V}_s(k) = \rho \int d^3r V_s(r) e^{i\mathbf{k}\cdot\mathbf{r}}$; correspondingly,

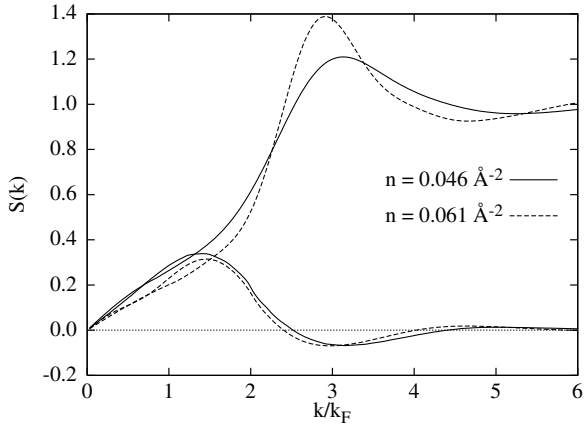

FIG. 1. The density structure functions $S(k)$ (upper curves) and correlation part of the spin structure functions $S_\sigma(k) - S_F(k)$ (lower curves) are shown at the densities $\rho = 0.046$ Å^{-2} (solid lines) and $\rho = 0.061$ Å^{-2} (dashed line). The zero level (dotted line) is included as a guide to the eye.

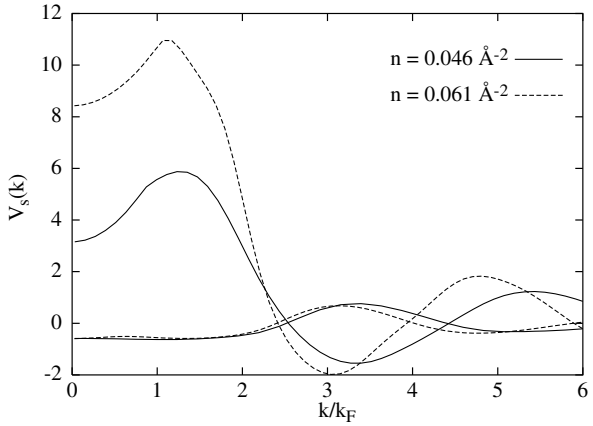

FIG. 2. The density-channel and spin-channel interactions obtained from the corresponding structure functions through the RPA relationship (3) are shown for the densities $\rho = 0.046$ Å^{-2} (solid lines) and $\rho = 0.061$ Å^{-2} (dashed lines). The interactions are given in units of $\hbar^2 k_F^2/2m$.

the Lindhard function has the dimension of an inverse energy. We note in passing that the RPA (4) also satisfies the m_1 sum rule as an identity, whereas the inclusion of at least two-particle–two-hole excitations is needed to satisfy higher-order sum rules [10].

The long-wavelength limit of $\tilde{V}_\rho(k)$ is related to the bulk compressibility

$$\frac{d}{d\rho}\rho^2\frac{dE}{d\rho} = \frac{d}{d\rho}\rho^2\frac{dE_F}{d\rho} + \tilde{V}_\rho(0+), \tag{5}$$

where E and E_F are the energy per particle of the interacting and the noninteracting systems, respectively. We can thus determine $\tilde{V}_\rho(0+)$ from the equation of state.

Figure 2 shows the effective interactions $\tilde{V}_s(q)$ defined through relations (3) and (4) at two representative densities. These effective interactions resemble the Aldrich-Pines pseudopotentials [11], which have been derived in a similar spirit. The most prominent features are the same: the density-channel interaction is repulsive and can lead to a zero sound excitation, whereas the spin-channel interaction does not. We also note that, similar to the spin-structure function, there is relatively little change in the spin-channel effective interaction when given in dimensionless units.

Getting back to the self-energy, we assume low-lying excitations. In that case, the so-called G0W approximation [9,12] for the self-energy,

$$\Sigma(k, E) = u(k) + i\sum_s (2s+1)\int \frac{d^2q\, d(\hbar\omega)}{\rho(2\pi)^3} G^0(\mathbf{k}-\mathbf{q}, E-\hbar\omega)\tilde{V}_s^2(q)\chi_s(q,\omega) \equiv u(k) + \Sigma^{(\rho)}(k, E) + \Sigma^{(\sigma)}(k, E), \tag{6}$$

should be appropriate. We have split the full self-energy into an energy-independent mean field term $u(k)$ and the two dynamic, energy-dependent portions $\Sigma^{(\rho)}(k, E)$ and $\Sigma^{(\sigma)}(k, E)$ originating from coupling to density and spin fluctuations, respectively. We have taken for $u(k)$ the exchange term of the static density-channel interaction $\tilde{V}_\rho(q)$. One could here, in principle, also use the single-particle spectrum of correlated basis functions theory, but the basic results are very similar and within the limits of the present description.

The self-energy is conveniently evaluated by Wick rotation in the complex ω plane; the salient features have been discussed in the literature [7,8,12]. With the stated approximations, one obtains the spectrum

$$\epsilon(k) = t(k) + \Sigma(k, \epsilon(k)). \tag{7}$$

In the numerical applications, we have used the "on-shell approximation" $\epsilon(k) \to t(k)$ in the self-energy. It is our experience in ^{3}He-^{4}He mixtures that this gives good agreement with much more sophisticated implementations of the same theory [13]. Especially, one might be led to "dress" the single-particle Green's functions in the self-energy (6) by solving Eq. (7). However, single-particle Green's functions appear in two locations: One is the external propagator spelled out explicitly in Eq. (6); the other location is the particle-hole propagator. To maintain the symmetry between "internal" and "external" propagators, one should apply any modifications either to both or to none. Using a nontrivial spectrum the particle-hole propagator is, on the other hand, extremely dangerous because one would then violate the m_0 and m_1 sum rules and, hence, modify the overall importance of the dynamic part of the self-energy in an uncontrolled way. A *systematic* improvement of the theoretical framework is the inclusion of *pair* excitations [14].

Figure 3 shows the mean field $u(k)$ and the dynamic contributions $\Sigma^{(\rho)}(k, t(k))$ and $\Sigma^{(\sigma)}(k, t(k))$. All three terms are, in the vicinity of the Fermi momentum, rather smooth functions of the single-particle momentum k. $u(k)$ has positive slope at the Fermi wave number and, hence, decreases the effective mass, whereas both dynamic contributions cause an effective mass enhancement. The S shape of the spin-channel term is typical for attractive interactions [7,8,15,16]. At higher momenta, we found similar structures as in three-dimensional ^{3}He originating from a coupling of the single-particle excitation to the maxon [7,8]; these will not be discussed here. The full on-shell self-energy is shown, for several densities, in Fig. 4. The most evident feature is the development of a saddle around the Fermi wave number, which is due to spin fluctuations and leads, at high densities, to an instability.

The effective mass is obtained from the single-particle spectrum through

$$\frac{\hbar^2 k_F}{m^*} \equiv \frac{d\epsilon(k)}{dk}\bigg|_{k=k_F}. \tag{8}$$

Both experiments [6,17,18] and our calculations indicate that the effective mass increases rapidly with density and eventually becomes singular. The primary quantity that one calculates is the single-particle spectrum. For a theoretical analysis, it is therefore more convenient to discuss the inverse, m/m^*. Figure 5 shows, as our final result, the density dependence of the effective mass ratio m/m^* and compares it with the experiments of Refs. [6,17,18]. The fluctuations of our results are due to the statistical uncertainties of the diffusion Monte Carlo simulations. These are most pronounced in the spin-dependent correlations since the spin-structure function, $S_\sigma(k) = S_{\uparrow\downarrow}(k) - S_{\uparrow\uparrow}(k)$, is the difference of two quantities obtained from diffusion Monte Carlo simulations, but these fluctuations do not affect our general result.

The overall theoretical picture is practically the same as the experimental one, although our theory overestimates the correlation effect somewhat and the instability occurs around 0.048 Å^{-2}. The experimental ratio m/m^* is, to reasonable accuracy, a linear function of the density which goes through zero between $\rho = 0.051$ Å^{-2} and $\rho = 0.07$ Å^{-2}, causing a singular m^*. Our theoretical calculations reproduce the experimental values within about 10%–20% when compared with the spectrum of the noninteracting Fermi gas. This is satisfactory considering the simplicity of the G0W approximation (6).

The individual contributions from spin and density fluctuations are also shown in Fig. 5. The mean field term and density fluctuations contribute somewhat less than spin fluctuations, but are non-negligible. Both effects are individually insufficient to reproduce the experimental values. This is the case in both two and three dimensions [8], but the relative importance of spin fluctuations appears to be larger in 2D.

In both three and two dimensions, one observes a divergence of the effective mass at some high density. Extrapolating the data of Refs. [19,20], one observes that the divergence of the effective mass would appear in 3D at a density 0.03 Å^{-3}, whereas the liquid-solid phase transition occurs at 0.023 Å^{-3}. The 2D situation is somewhat different: Reference [6] implies a divergence of m^* at about 0.051 Å^{-2}; earlier data [17,18] suggest a somewhat higher density. The film freezes between 0.052 Å^{-2} [6] and 0.063 Å^{-2} [21].

It seems unlikely that freezing and the singularity of the effective mass have the same cause. The divergence in m^* is due to the increasing importance of spin fluctuations

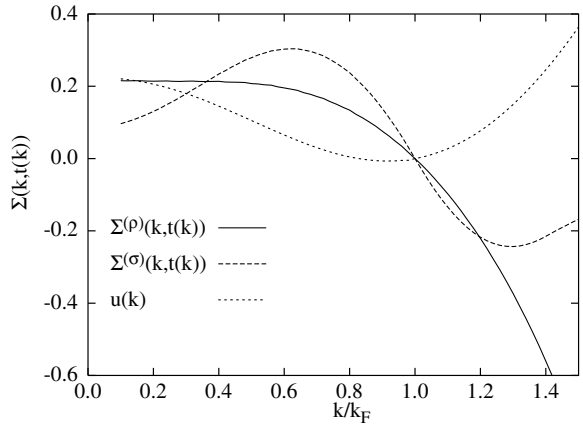

FIG. 3. The figure shows the Fock term $u(k)$ (short-dashed line), the "density" term $\Sigma_\rho(k, t(k))$ (solid line), and the "spin" term $\Sigma_\sigma(k, t(k))$ (long-dashed line) of the self-energy for the density $\rho = 0.046$ Å^{-2}. All functions have been shifted to be zero at the Fermi momentum; all energies are given in units of $\hbar^2 k_F^2/2m$.

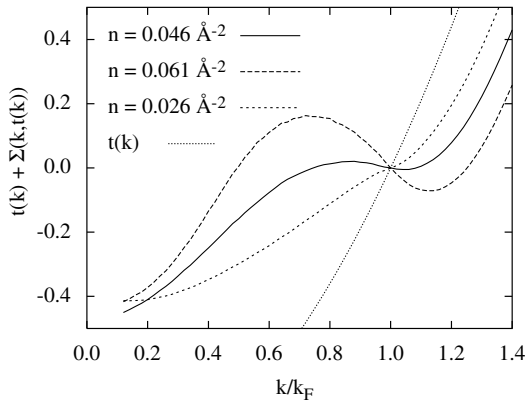

FIG. 4. The figure shows the full on-shell spectrum (7) for the densities $\rho = 0.026$ Å^{-2}, $\rho = 0.046$ Å^{-2}, and $\rho = 0.061$ Å^{-2}. The free single-particle spectrum $t(k)$ is also shown for comparison. All functions have been shifted to be zero at the Fermi momentum; all energies are given in units of the Fermi energy of the noninteracting liquid.

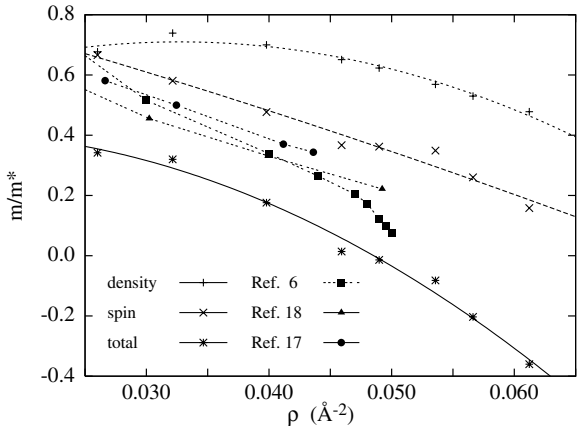

FIG. 5. The figure shows the density dependence of m/m^* at the Fermi wave number k_F (solid line). Also shown are the results from density fluctuations (long-dashed line) and from spin fluctuations only (short-dashed line). The dashed lines with solid markers show the experimental values of Refs. [6,17,18]. The lines through the theoretical data are quadratic fits.

with density. This is manifested very clearly in 2D and also visible in 3D. The theory used here reproduces those features, in both 3D and 2D, at a semiquantitative level without the need for phenomenological input. The fact that we obtain a negative slope of the single-particle spectrum is clearly a consequence of the G0W approximation; a self-consistent theory should not have solutions for unstable situations. Nevertheless, relatively simple approximations have often shown the same physics as more sophisticated theories in the stable regime, which then simply cease to have solutions beyond the point of an instability. We are presently not prepared to speculate on "what is beyond" the singularity.

A second interesting question is why the 2D theory apparently overestimates the effective mass, whereas it underestimates m^* in 3D. One can only speculate that a 2D model is an obvious simplification of the real physical situation of an adsorbed film, and little is known about the severity of such an approximation for ^{3}He.

We have shown that understanding the value of the effective mass in two-dimensional ^{3}He is — in analogy to the more common three-dimensional case — not a simple problem, and simple paradigms that try to attribute the effect to a single cause are genuinely inadequate. Both spin and density fluctuations have profound effects, although spin fluctuations are stronger in 2D and we are more inclined to associate the effect of density fluctuations to Feynman-Cohen backflow instead of "localization." We hesitate to conclude that the flattening of the single-particle spectrum caused by interactions should be identified with a Mott transition; it indicates more likely a lack of self-consistency of our calculations. The observed singularities [6,17,18] that depend sensitively on the underlying substrate structure are most likely caused by it. Quantitative improvement will first be sought in a more accurate description of the response functions [14].

This work was supported, in part, by the Austrian Science Fund under Project No. P12832-TPH and from DGI (Spain) Grant No. BFM2002-00466 and Generalitat de Catalunya Grant No. 2001SGR-00222.

[1] J. Casulleras and J. Boronat, Phys. Rev. Lett. **84**, 3121 (2000).
[2] V. Grau, J. Boronat, and J. Casulleras, Phys. Rev. Lett. **89**, 045301 (2002).
[3] N. F. Berk and J. R. Schrieffer, Phys. Rev. Lett. **17**, 433 (1966).
[4] S. Doniach and S. Engelsberg, Phys. Rev. Lett. **17**, 750 (1966).
[5] D. Vollhardt, Rev. Mod. Phys. **56**, 99 (1984).
[6] A. Casey, H. Patel, J. Nyéki, B. P. Cowan, and J. Saunders, Phys. Rev. Lett. **90**, 115301 (2003).
[7] B. L. Friman and E. Krotscheck, Phys. Rev. Lett. **49**, 1705 (1982).
[8] E. Krotscheck and J. Springer, J. Low Temp. Phys. **132**, 281 (2003).
[9] A. L. Fetter and J. D. Walecka, *Quantum Theory of Many-Particle Systems* (McGraw-Hill, New York, 1971).
[10] V. Apaja, J. Halinen, V. Halonen, E. Krotscheck, and M. Saarela, Phys. Rev. B **55**, 12 925 (1997).
[11] C. H. Aldrich and D. Pines, J. Low Temp. Phys. **25**, 677 (1976).
[12] B. L. Friman and J. P. Blaizot, Nucl. Phys. **A372**, 69 (1981).
[13] E. Krotscheck, J. Paaso, M. Saarela, K. Schörkhuber, and R. Zillich, Phys. Rev. B **58**, 12 282 (1998).
[14] E. Krotscheck and K. Schöorkhuber, Physica (Amsterdam) **320B–333B**, 102 (2003).
[15] G. E. Brown, C. J. Pethick, and A. Zaringhalam, J. Low Temp. Phys. **48**, 349 (1982).
[16] V. K. Mishra, G. E. Brown, and C. J. Pethick, J. Low Temp. Phys. **52**, 379 (1983).
[17] D. S. Greywall, Phys. Rev. B **41**, 1842 (1990).
[18] K.-D. Morhard, C. Bäuerle, J. Bossy, Y. Bunkov, S. N. Fisher, and H. Godfrin, Phys. Rev. B **53**, 2658 (1996).
[19] D. S. Greywall, Phys. Rev. B **27**, 2747 (1983).
[20] D. Greywall, Phys. Rev. B **33**, 7520 (1986).
[21] C. Bäuerle, Y. M. Bunkov, A. S. Chen, S. N. Fisher, and H. Godfrin, J. Low Temp. Phys. **110**, 333 (1998).